A battery-free wearable system for on-device human activity recognition using kinetic energy harvesting

Milan Deumer[†1], Moid Sandhu[†2], Sara Khalifa[3], Brano Kusy[3], Kai Geissdoerfer[4],
Marco Zimmerling[5], Raja Jurdak[6]

[1]Fraunhofer Heinrich Hertz Institute, Berlin, Germany; [2]Australian e-Health Research Centre, Health & Biosecurity,
Commonwealth Scientific and Industrial Research Organisation (CSIRO), Brisbane, Australia; [3]Data61, CSIRO,
Brisbane, Australia; [4]TU Dresden, Dresden, Germany; [5]TU Darmstadt, Darmstadt, Germany; [6]Queensland
University of Technology, Brisbane, Australia

milan.deumer@gmail.com, moid.sandhu@csiro.au, sara.khalifa@data61.csiro.au,
brano.kusy@data61.csiro.au, kai.geissdoerfer@tu-dresden.de,
marco.zimmerling@tu-darmstadt.de, r.jurdak@qut.edu.au

Abstract

Wearable devices are increasingly prevalent in daily life, especially for activity recognition, health monitoring, and fitness management. However, their reliance on batteries poses inconveniences, expenses, and environmental issues. To address these concerns, we present a battery-free wearable system that utilizes kinetic energy from human activities as both the energy source and a sensing signal for on-device activity recognition. With a carefully designed hardware and software, our system achieves real-time activity recognition on an ultra-low-power micro-controller, including on-board classification and wireless transmission. Real-world experiments demonstrate that our system operates the wearable device up to 95.2 % of the time, inferring and reporting ongoing activities within 8 seconds with up to 87 % accuracy.

Categories and Subject Descriptors

I.2.11 [**Artificial Intelligence**]: Distributed Artificial Intelligence

General Terms

Machine Learning, Human Activity Recognition

Keywords

Wearable, Battery-free, Low power, Kinetic energy harvesting

1 Introduction

With recent technology advancements, smart wearable devices are becoming increasingly important in various fields of the Internet of Things (IoT) including human-centric applications like health assessment [1] and activity recognition [2, 3]. A major issue with current wearable devices is their batteries, which cannot provide sustained operation due to finite energy storage capacity. Batteries are subject to a limited lifetime, a limited number of charging cycles, and aging effects. In addition, batteries are costly, bulky, and hazardous for the environment, which impedes the widespread adoption of wearable devices and increases their environmental footprint [4].

To overcome these issues, energy harvesting is a promising solution that converts ambient energy into electrical energy to power wearable IoT devices. Various sources of ambient energy can be exploited depending on the application, such as solar, kinetic, thermal, and high-frequency electromagnetic waves. In addition, energy harvesting can simultaneously provide context information, simplifying the sensor design and improving efficiency [2, 5].

Challenge. Battery-free IoT devices powered by energy harvesting face the challenge of scarce, time-varying, and often unpredictable ambient energy availability. This requires the devices to operate solely on the energy it extracts from the environment and cope with intermittency (frequently turning on and off) caused by the irregular and discontinuous energy supply [6]. Therefore, advanced signal processing or machine learning algorithms running on the devices are needed to achieve energy efficiency by avoiding transmitting large amounts of raw sensor data using the power-hungry radio.

Contribution. We demonstrate the design and implementation of a fully battery-free wearable system that performs real-time on-device human activity recognition, shown in Fig. 1. Our system uses kinetic energy harvesting in the form of a piezoelectric transducer to capture energy from the human heel strike and also to provide the sensing signal for activity recognition. To maximize energy input while providing a high-quality, reliable sensing signal, we optimize key tuning parameters of the harvester and design a dedicated energy management architecture. We collect data from five human subjects performing common human activities (walk-

---

[†] Both authors contributed equally in this work.

(b) Piezoelectric transducer

(c) Energy harvester and data transmitter

(a) Hardware prototype
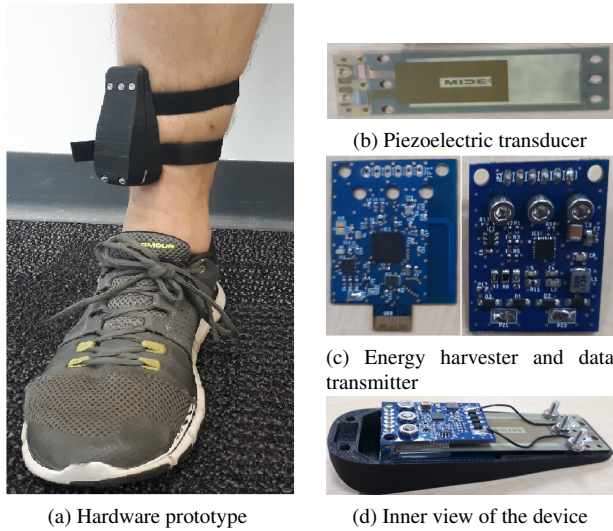

(d) Inner view of the device

Figure 1: Our system integrates all components required for battery-free on-device human activity recognition in a small and lightweight wearable device.

Table 1: Comparison of this paper with prior work.

Work	Battery-free	Sensing using EH	On-device classification
[2, 5, 7–10]	✗	✓	✗
[11]	✗	✓	✓
[12, 13]	✓	✗	✗
[14]	✓	✓	✗
This work	✓	✓	✓

ing, running, jumping, going up/down the stairs) and train four widely-used machine learning algorithms for human activity recognition. Using this empirical data, we demonstrate that our system can execute the end-to-end activity recognition pipeline, including signal acquisition, feature extraction, classification, and wireless transmission of the inferred activity in real time on an ultra low-power microcontroller while relying only on energy harvested during the activity.

2 Related Work

Prior work considers diverse energy sources for battery-free wearable devices, such as solar [11], thermal [15], radio frequency [16], and human motion [17]. The latter is a particularly promising energy source as users typically wear the devices for extended periods during daily activities, allowing for self-powering by harvesting energy from body movements. Specialized transducers (i.e., piezoelectric [12], triboelectric [18], or electromagnetic [17]) are needed to convert the kinetic energy into electric energy. Piezoelectric transducers are a popular choice due to their simplicity and compatibility with microelectromechanical systems [13].

Although prior work [2, 5, 7–11, 14] has greatly advanced the research towards battery-free wearable devices, many of these studies still use batteries and do not demonstrate fully self-sustained operation. For example, the most related study implements a battery-free wearable system using kinetic en-
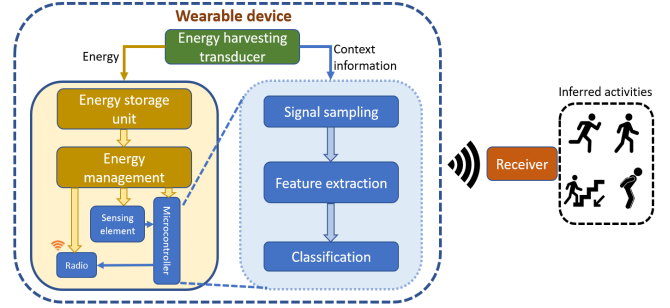

Figure 2: Overview of our battery-free wearable system for on-device human activity recognition.

ergy harvesting for human activity recognition, but does not demonstrate on-device activity classification [14].

To our knowledge, there is no prior research that achieves on-device battery-free activity recognition. Table 1 summarizes and compares previous studies by the aforementioned criteria. It can be seen that this paper is the first to showcase a complete end-to-end system that is battery-free, relies entirely on harvested energy from human motion for both sensing and energy generation, and is capable of executing the entire activity recognition pipeline on the device, thus achieving autonomous and real-time operation.

3 System Design

This section describes the design of the first battery-free system for on-device human activity recognition. Fig. 2 provides a high-level overview for our system design. The activity recognition pipeline runs on a battery-free device, which is powered by the energy harvested from human motion. The harvested energy is first stored in an energy storage unit. An energy management unit uses the stored energy to power various hardware components, including microcontroller, sensing circuit, and radio. Fig. 2 shows that the harvesting signal is also used for activity recognition using standard techniques for signal processing, feature extraction, and classification. Finally, the inferred activity is sent to a nearby receiver using a low-energy wireless protocol.

In the following, we outline the hardware and software components of our design and their respective roles in addressing the challenges that arise from battery-free operation. We investigate tuning methods to optimize the energy yield from the piezoelectric transducer and compare various energy-harvesting architectures to maximize the transfer of power from the transducer to the system. We present an efficient current sensor design to extract a high-fidelity activity signal while simultaneously harvesting energy from the transducer. Finally, we integrate these components into a compact battery-free device for human activity recognition.

3.1 Transducer tuning

We use a MIDÉ Technology[1] S230-J1FR-1808XB piezoelectric bending transducer (71 mm × 25.4 mm) with a natural resonant frequency of 130 Hz. To extract the most energy with this transducer we attach our device to the leg/ankle to
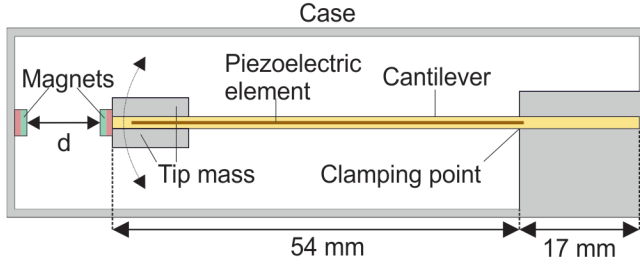
---

[1] https://www.mide.com/

Figure 3: Tuning the piezoelectric transducer using clamping, tip mass, and magnets. The mass is attached to the tip of the cantilever and two magnets are used for further tuning.
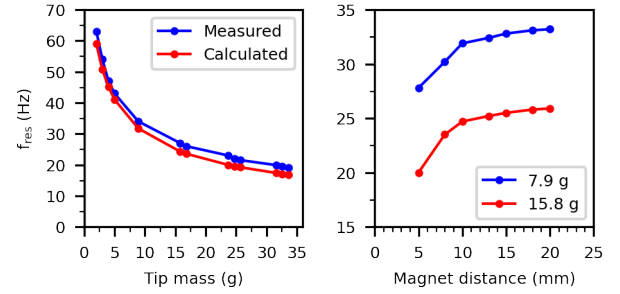

Figure 4: Left: The resonant frequency exhibits an inverse linear relationship with the tip mass and matches the calculated values well. Right: For the magnet tuning, a steep decrease in resonant frequency is observed for both tip masses when reducing the distance between the two magnets.

efficiently capture the heel-strike energy. Nevertheless, we still need to tune the resonance frequency of the transducer to optimize the energy yield [19].

Most of the energy in the power spectrum of human motion lies in the spectral range below 10 Hz [19]. thus, to efficiently capture the heel-strike energy and obtain a high-quality sensing signal, we must shift the resonant frequency of our transducer from 130 Hz closer to the 10 Hz range.

Fig. 3 illustrates three key methods to decrease the resonant frequency of a bending piezoelectric transducer: (1) repositioning the clamping point to increase the effective length of the cantilever, (2) attaching a mass to the tip of the transducer to dampen the oscillation, and (3) mounting a magnet on the tip of the beam and placing another static magnet with opposite polarity at a small fixed distance [20].

Clamping point. To achieve the lowest resonant frequency, we choose the lowest clamping point provided by our cantilever, which has the longest effective beam length.

Tip mass tuning. To characterize the influence of tip mass and magnet tuning, we connect the cantilever to a load shaker[2] and excite it with frequencies from 10 to 60 Hz. The open-circuit voltage V_{oc} and the short circuit current I_{sc} are measured with a multi-meter. The left side of Fig. 4 shows the measured resonant frequency of the transducer for varying tip masses and the corresponding values obtained using the transducer's datasheet. We find that tip mass tuning alone is insufficient, so magnet tuning should be explored to further decrease the resonant frequency without significantly increasing the size and weight of the transducer.

Magnet tuning. We mount one magnet to the tip of the cantilever and one magnet of opposite polarity to a screw that allows altering the distance between the magnets. We use a 3 mm thick neodymium magnet with a 12 mm diameter attached to the transducer, which keeps the moving part of the harvesting system compact. We use a 5 mm thick ceramic magnet with a 12 mm diameter as static magnet. The right-hand side of Fig. 4 shows the transducer's resonant frequency for varying distances between the magnets and two different tip masses. For small distances between the magnets, the resonant frequency of the transducer decreases significantly.

Implications on system design. Our results show that the

largest possible tip mass and the lowest possible magnet distance would be best to achieve a low resonant frequency. However, to maintain a compact size and a stable operation without damaging the device, we need to strike a balance between weight/size of the tip mass and the inter-magnet distance. We therefore select a tip mass of 12.5 g and an inter-magnet distance of 5 mm. This choice significantly reduces the resonant frequency of the transducer from 130 Hz to 22 Hz, while providing a stable and compact packaging.

3.2 Energy management and storage

To harvest energy from the transducer, its output signal has to be rectified and then used to accumulate energy in a storage capacitor. Since ambient energy varies over time and is often insufficient to enable continuous operation of the device, an energy management unit (EMU) is necessary.

The EMU controls the operation of its output voltage regulators, which provide the supply voltage for the other system components depending on the voltage on the mstorage capacitor. A key design decision here is whether to use an EMU with a boost converter [21] at its input.

Using a boost converter allows to regulate the input voltage of the EMU to a specified value. This enables Maximum Power Point Tracking (MPPT), where the voltage is regulated to the Maximum Power Point (MPP) of the source to most efficiently extract energy from the transducer. This, however, only works if the input excitation changes only slowly over time and and if the boost converter can regulate the input to the MPP voltage level. In our case, the harvesting signal comes in strong, isolated bursts caused by the human heel strike and open-circuit voltages of up to 6.6 V. Therefore, it is challenging for a boost converter to regulate to a MPP. Thus, for our application, we find a buck-only architecture is up to 30 % more efficient than a buck-boost architecture.

We choose a Linear Technology LTC3588 EMU, which turns its output regulators on at a voltage of about 4 V on the storage capacitor and shuts them down when the voltage drops below 2 V. Using a 220 μF capacitor, the energy stored in this voltage range is sufficient to guarantee a minimum uninterrupted execution of 2 s per charging cycle.

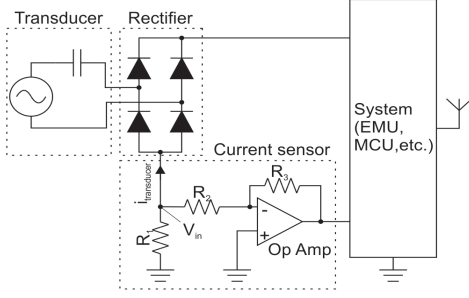[2]https://controlledvibration.com/product-item/1lb-load-shaker/

Figure 5: The sensing mechanism using energy harvesting current. The low-side energy harvesting current sensor is comprised of a shunt resistor in the return path of the rectifier and an inverting amplifier.

3.3 Harvesting-based activity sensor

A central component of our proposed system is the motion sensor that detects the wearer's movements. While accelerometers are commonly used for this purpose, recent studies demonstrate that piezoelectric transducers can be used to classify human activities more energy efficiently [5, 7, 22]. In particular, the harvester current signal has been found to be suitable for activity classification. Therefore, we opted to incorporate a current sensor into our system, which converts the harvesting current to a voltage signal that can be sampled using an analog-to-digital converter (ADC).

We propose a shunt-meter circuit based on an inverting operational amplifier, illustrated in the "Current sensor" box in Fig. 5. By placing the current sensor in the return path of the rectifier (low-side sensor), it is not directly exposed to the harvesting voltage. As a result, the amplifier can be powered with a supply voltage lower than the harvesting voltage and high common-mode voltages can be eliminated.

Using a Renesas ISL28194 operational amplifier[3] with resistor values of $R_1 = 10\,\Omega$, $R_2 = 330\text{k}\Omega$, and $R_3 = 20\text{M}\Omega$, the transimpedance is $r = 606.06\,\text{V/A}$ at a bandwidth of $58\,\text{Hz}$ and a quiescent current of only $330\,\text{nA}$. This enables sampling of current signals with amplitudes of up to $2\,\text{mA}$, which is the maximum amplitude occurring during our experiments, and frequencies of up to $29\,\text{Hz}$, which is well above the $22\,\text{Hz}$ resonant frequency of our tuned transducer.

3.4 Processing and runtime operation

We use a Nordic Semiconductor nRF52840 wireless microcontroller[4] to sample and process the sensor data and control the radio interface because of its low power consumption and various sleep modes. In addition, the integrated low-power radio interface eliminates the need for inter-chip communication between the microcontroller and the radio, further reducing overall power consumption.

The microcontroller samples the harvesting signal using the on-board 12-bit ADC at a rate of $124\,\text{Hz}$. After the completion of a pre-defined sampling window, the system computes features and runs the classification algorithm. Finally, the classification result is encoded as a 4 byte payload in a

16 byte packet, which is transmitted using a proprietary protocol by Nordic Semiconductor in a connection-less (broadcast) mode at a data rate of $2\,\text{Mbit/s}$.

3.5 Prototype

Fig. 1 shows the current prototype of our system. The device uses a piezoelectric transducer for energy harvesting (Fig. 1b). To ensure a compact and lightweight design, the device is divided into two Printed Circuit Boards (PCBs) that are mounted on both sides of the piezoelectric transducer (Fig. 1c). The first printed circuit board (PCB) contains the EMU, rectifier diodes, energy storage capacitor, and current sensing circuit. The second PCB hosts the wireless microcontroller and the antenna for data transmission. The neodymium magnet is attached to the front tip of the piezoelectric cantilever. To attach the device to the user's leg, we design and manufacture a custom 3D-printed casing (Fig. 1d). The casing includes a frame for securely placing the static magnet and slots for velcro strips to ensure comfortable strapping of the device to the user's leg (Fig. 1a).

4 Evaluation

This section describes the evaluation of our system covering the data collection campaign and the on-device human activity recognition performance as well as the energy consumption, energy harvesting, and intermittency analysis.

4.1 Data collection

We use our system to collect KEH data[5] from five adult and healthy participants during four common human activities: walking, running, jumping, and going up/downstairs. The participants are 20–60 years of age and their weight ranges from 50 to $100\,\text{kg}$. Each participant performs all four activities six times with a duration of $62\,\text{s}$ per activity.

We conduct two separate sets of experiments. In the first set, the wearable device transmits only raw KEH data in $2\,\text{s}$ windows. Later, this data is used to train machine learning algorithms offline as described in 4.2. In the second set of experiments, the developed decision tree classifier is implemented on the sensor node which runs solely using the harvested energy from human movements and transmits the inferred activity after every $8\,\text{s}$. The hardware prototype for collecting and transmitting the data is attached to the lower part of the user's leg using velcro straps as depicted in Fig. 1a. The receiver is placed in close proximity to the transmitter for collecting real-time KEH data during the experiments. The human activities are labeled manually, which serves as ground truth during the training of the machine learning classification algorithms.

4.2 Human activity recognition

We use the collected data to assess the performance of human activity recognition with our battery-free prototype using standard mechanism of signal processing, feature extraction, and machine learning classification.

Methods. First, we partition the data into different window sizes ranging from 1 to $10\,\text{s}$, and extract 21 time-domain features from these windows. We split the data into 80–20 % ratio for training and testing the model respectively.
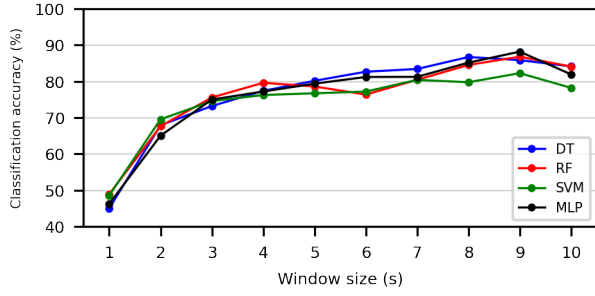

Figure 6: The average accuracy of the four considered classification algorithms for varying window sizes It can be observed that the accuracy increases with increasing window sizes up to 8 s, beyond which there is no significant improvement in accuracy.

We train four commonly used machine learning classification models using ten-fold cross-validation: Decision Tree (DT), Random Forest (RF), Support Vector Machine (SVM), and Multi-Layer Perceptron (MLP). For each type of classifier, we explore the performance with different model hyperparameters. We repeat the training process for various window sizes and different subsets of features, chosen based on the feature importance metric.

We further evaluate the average time needed to classify a sample for each type of classifier as the energy cost of the machine learning algorithm is proportional to the number of system operations and the classification execution time. This is done by measuring the time it takes to classify all available samples, divided by the total number of samples.

Results. We evaluate the trained classifiers based on their average accuracy on the test sets. We select the best performing classifier and window size from the scanned parameters and present the results in Fig. 6. As shown in Fig. 6, the activity recognition accuracy increases with the window sizes for all classifiers. However, the improvement becomes less significant for larger windows (>8 s). This is because smaller window sizes provide little information about the activity being performed since only a few, if any, steps are captured in the window. As the window size increases, the information content per sample increases, but since most activity patterns in the considered activities last only up to a few seconds, the information gain saturates after 8 s windows.

We also find that all classifiers offer similar performance, with peak accuracies around 87 % for an 8 s window, which is significantly higher than the most closely related KEH-based off-device activity recognition system, that achieves an accuracy of less than 60 % for the same 8 s window size [14].

Due to its simple architecture, the DT shows 5–15× faster computation times compared to the other classifiers, which corresponds to the lowest power consumption on the device. Thus, we find this classifier to be the best for our scenario.

Fig. 7 shows the confusion matrix of the DT classifier on the previously unseen test dataset. We observe that there is higher confusion between the activities of walking and going up/downstairs. This is an intuitive finding since both activities are very similar and are mainly distinguished by the spa-

Figure 7: The confusion matrix of the Decision Tree (DT) classifier for a window size of 8 s.

cial direction, which is difficult to determine from the harvested signal of a single-axis piezoelectric cantilever. This appears to be a general limitation of human activity recognition based on kinetic energy harvesting signals [5].

4.3 Energy consumption

The total power consumption of our system is the sum of the contributions of the energy management unit P_{EMU}, the current sensor P_{Sens}, and the microcontroller and radio P_{MCU}.

Methods. We measure P_{MCU} using an Otii Ace[6]. The device is set up to supply a voltage of 1.8 V and measures the current drawn by the sensor node as well as the voltage at its clamps. From the recorded traces, we can calculate the energy required for the execution of each task of the microcontroller. The power consumption of the EMU and the sensor, however, can only be estimated as both the voltage and current drawn by the EMU and the sensor depend on the current state of the storage capacitor and the vibration intensity applied to the transducer. Therefore, we use the average harvested current during our experiments together with circuit analysis and the quiescent currents of the EMU and sensor listed in their datasheets to analytically estimate the energy consumption of these components.

Results. From the measurements with the Otii Ace, we find the energy costs to turn the microcontroller on, collect a single sample, and transmit the inferred activity are 72.84 μJ, 1.07 μJ, and 39.71 μJ. The respective power consumption then depends on the sampling frequency and window size. Using the quiescent current of the EMU provided in its datasheet[7] and assuming the main storage capacitors voltage to be always between the turn-off threshold (2.9 V) and the maximum rated voltage of the capacitor (6.3 V), we estimate the EMU's average power consumption to be between $P_{EMU,min} = 2.79\,\mu W$ and $P_{EMU,max} = 5.99\,\mu W$. The power consumption of the sensor also depends on the transducer current. Therefore we calculate the average current from the traces recorded during the experiments described in Sec. 4.1. We find the average current to be $I_{td,av} = 60.43\,\mu A$, which results in an average power dissipation of $P_{Sens} = 633.82\,nW$.

---

[6] https://www.qoitech.com/otii-ace/
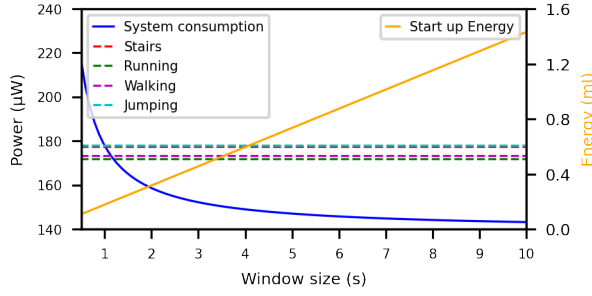[7] https://www.analog.com/media/en/technical-documentation/data-sheets/35881fc.pdf

Figure 8: The average power consumed (solid line) and harvested energy (dashed lines) by our device to perform one execution cycle. For window sizes greater than 1.2 s, the average harvested power exceeds the consumed power.
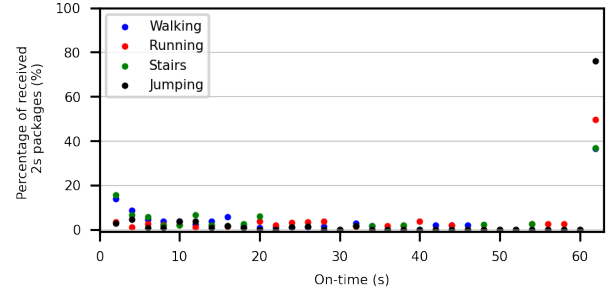

Figure 9: The percentage of received 2 s packets over the length of the operating period they were part of. The majority of packets arrive as part of 62 s operating periods, which corresponds to continuous operation throughout the activity duration.

Fig. 8 shows the total average power consumption of the system after start-up, which is dependent on the window size, as well as the energy required to execute a full cycle, including start-up. As the window size increases, the average power consumption approaches that of the sampling task, while the cycle energy increases linearly. Therefore, if there is consistent but low energy harvesting input that exceeds the system's average consumption, using a longer window size can maximize the system's on-time. On the other hand, if the harvested power level is below the average system power consumption or the harvesting patterns are highly irregular, using a short window size can ensure that the system executes at least one full cycle every time it is turned on.

4.4 Energy harvesting

This section describes the average power harvested by our proposed system during various human activities.

Methods. We compute the harvested power P_{In} as the product of harvested transducer current I_{td} and the storage capacitor voltage U_{Cap}. From the experiments described in Sec. 4.1, we collected traces of the current flowing into the device. For the capacitor voltage, we again use the lower boundary estimation of $U_{Cap,min} = 2.9\,\text{V}$. Thus, a lower boundary of the average harvested power $P_{In,min}$ can be calculated as $P_{In} = I_{td} \cdot U_{Cap}$.

Results. Fig. 8 shows the estimated values of the harvested (horizontal lines) and consumed power of the system during the four activities. From this figure, we find that the average harvested power lies above the consumed power of the system for all activities for window sizes greater than about 1.2 s. Thus, our proposed system can run battery-free activity classification after accumulating energy for at least 1.2 s.

4.5 Intermittency

In practice, the harvested power is not constant over time but rather comes in short bursts caused by the heel strike. Consequently, the system may still run out of energy if the break between two such strikes is too long, even if the average harvested power is greater than the system's power consumption. Therefore, the consecutive on-time of the system is another important measure to evaluate the performance of a battery-free sensor node, which also offers insights into suitable window sizes for the application at hand.

Methods. By analyzing the timestamps of received packets from Sec. 4.1 experiments, it's possible to determine when the sensor node was operating and charging up. The device transmits a radio packet every two seconds during data collection, which means that each received packet represents two seconds of operation. If two consecutive packets have timestamps that are exactly two seconds apart, it indicates continuous operation over that time period. Although packets may be lost due to radio link issues, this method can provide a lower boundary of the on-time of the sensor, quantized to two-second periods.

Another metric that can be derived from this evaluation is the coverage, which is the ratio of on-time to total activity time for different window sizes. Only on-time periods that fit a full window are considered, and a four-second period of operation would be considered as four seconds of on-time for window sizes of two and four seconds, and three seconds for a three-second window size. Larger window sizes aren't considered as the sensor would have turned off before acquiring a full window.

Results. After analyzing the timestamps of received packets as described above, we plot the distribution of operating periods in Fig. 9 for all four activities. The figure shows the percentage of packets received over the sensor's operating period during which the packets were received. The analysis of the harvested energy in Sec. 4.4 suggests that the sensor should be able to operate continuously when transmitting results every 2 s, as is the case in this experiment.

Looking at the histograms, we see that for each activity, the sensor operates continuously for a significant amount of time over the full course of the activity, indicated by an on-time of 62 s. This is especially pronounced for high-intensity activities like running and jumping. However, as suspected earlier, there are also packets received for shorter on-times due to insufficient energy. This is particularly visible for the lower-paced activities of going up/down stairs and walking, but also for jumping when heel strikes are weak or have long gaps between them.

Fig. 10 shows the coverage obtained during the experiments over window sizes between 2 and 10 s. As expected from the previous results, the coverage is lower for the low-
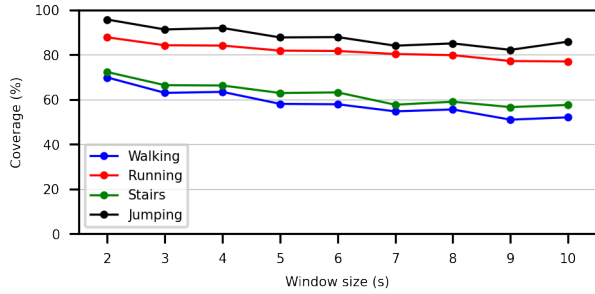
Figure 10: The average coverage of the sensor over various window sizes. It is observed that with a larger window size, the time required for recharging the capacitor after a shutdown also increases, resulting in a decrease in coverage.

intensity activities walking and going up/downstairs. When there is insufficient harvested energy, at least one packet is lost, even if the sensor is operating continuously most of the time. Therefore, small energy shortages have a greater impact on larger window sizes, as shown by the coverage values decreasing for every activity as the window size increases.

5   Conclusions

This paper showcases the first battery-free wearable system for on-device human activity recognition using kinetic energy harvesting. The system harvests energy from various human activities using a piezoelectric transducer and uses the same energy harvesting signal for activity recognition. To maximize the harvested energy, we tune the resonance frequency of the transducer using an experimentally explored combination of a magnet and a tip mass. We implement the entire activity recognition pipeline in real-time on an ultra low-power microcontroller while relying only on energy harvested during the activity. After rigorous experiments with different sampling rates and window sizes, we find that a decision tree classifier is best suited for our application with an accuracy of 87 % at a window size of 8 s, offering real-time activity recognition for up to 95.2 % of the time.

The design process highlights the importance of tailoring each component of the system to the specific application, which may also require rethinking commonly accepted methods. For example, although the use of buck-boost systems and MPPT is generally assumed to be the most efficient way to harvest energy, for our application with its specific constraints a buck-only architecture has shown superior performance. In the future, multi-source energy harvesters (e.g., solar, kinetic, thermal, RF) can be explored as simultaneous sources of energy and context information for ensuring perpetual and autonomous operation of the wearable device.

6   Acknowledgments

7   References

[1] S. Majumder et al. Wearable sensors for remote health monitoring. *Sensors*, 17(1):130, 2017.

[2] M. M. Sandhu et al. Solar: Energy positive human activity recognition using solar cells. In *2021 IEEE International Conference on Pervasive Computing and Communications (PerCom)*, pages 1–10. IEEE, 2021.

[3] M. M. Sandhu et al. Fusedar: Energy-positive human activity recognition using kinetic and solar signal fusion. *IEEE Sensors Journal*, 2023.

[4] J. Hester and J. Sorber. The future of sensing is batteryless, intermittent, and awesome. In *Proceedings of the 15th ACM Conference on Embedded Network Sensor Systems*, pages 1–6, 2017.

[5] S. Khalifa et al. Harke: Human activity recognition from kinetic energy harvesting data in wearable devices. *IEEE Transactions on Mobile Computing*, 17(6):1353–1368, 2017.

[6] Brandon Lucia et al. Intermittent computing: Challenges and opportunities. *2nd Summit on Advances in Programming Languages (SNAPL 2017)*, 2017.

[7] M. M. Sandhu et al. Towards energy positive sensing using kinetic energy harvesters. In *2020 IEEE International Conference on Pervasive Computing and Communications (PerCom)*, pages 1–10. IEEE, 2020.

[8] G. Lan et al. Capsense: Capacitor-based activity sensing for kinetic energy harvesting powered wearable devices. In *Proceedings of the 14th EAI International Conference on Mobile and Ubiquitous Systems: Computing, Networking and Services*, pages 106–115, 2017.

[9] Y. Han et al. A self-powered insole for human motion recognition. *Sensors*, 16(9):1502, 2016.

[10] H. Huang et al. Tribomotion: A self-powered triboelectric motion sensor in wearable internet of things for human activity recognition and energy harvesting. *IEEE Internet of Things Journal*, 5(6):4441–4453, 2018.

[11] M. Magno et al. Infiniwolf: Energy efficient smart bracelet for edge computing with dual source energy harvesting. In *2020 Design, Automation & Test in Europe Conference & Exhibition (DATE)*, pages 342–345, 2020.

[12] Q. Huang et al. Battery-free sensing platform for wearable devices: The synergy between two feet. In *2016 IEEE International Conference on Computer Communications*, pages 1–9. IEEE, 2016.

[13] Y. Kuang et al. Energy harvesting during human walking to power a wireless sensor node. *Sensors and Actuators A: Physical*, 254:69 – 77, 2017.

[14] P. Mayer et al. Energy-positive activity recognition-from kinetic energy harvesting to smart self-sustainable wearable devices. *IEEE Transactions on Biomedical Circuits and Systems*, 2021.

[15] B. Lee et al. High-performance compliant thermoelectric generators with magnetically self-assembled soft heat conductors for self-powered wearable electronics. 11(1), 2020.

[16] V. Talla et al. Wi-fi rf energy harvesting for battery-free wearable radio platforms. In *2015 IEEE International Conference on RFID (RFID)*, pages 47–54, 2015.

[17] S. Chamanian et al. Wearable battery-less wireless sensor network with electromagnetic energy harvesting system. *Sensors and Actuators A: Physical*, 249:77–84, 2016.

[18] Y. Song et al. Wireless battery-free wearable sweat sensor powered by human motion. *Science Advances*, 6(40):eaay9842, 2020.

[19] B. Maamer et al. A review on design improvements and techniques for mechanical energy harvesting using piezoelectric and electromagnetic schemes. *Energy Conversion and Management*, 199:111973, 2019.

[20] M. Magno et al. Kinetic energy harvesting: Toward autonomous wearable sensing for internet of things. In *2016 International Symposium on Power Electronics, Electrical Drives, Automation and Motion (SPEEDAM)*, pages 248–254. IEEE, 2016.

[21] K. Geissdoerfer et al. Shepherd: A portable testbed for the batteryless iot. In *Proceedings of the 17th Conference on Embedded Networked Sensor Systems*, pages 83–95, 2019.

[22] G. Lan et al. Entrans: Leveraging kinetic energy harvesting signal for transportation mode detection. *IEEE Transactions on Intelligent Transportation Systems*, 2019.